Accepted Manuscript

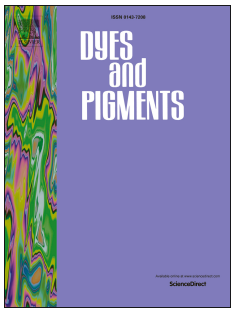

Modifying the *meso*-phenyl with electron donating amino groups strongly enhances BODIPY's ability as good singlet oxygen photosensitizer

Wenbin Hu, Xian-Fu Zhang, Xulin Lu, Shuai Lan, Dandan Tian, Tingting Li, Liangxia Wang, Siwen Zhao, Mingna Feng, Jing Zhang

PII: S0143-7208(17)31613-3

DOI: 10.1016/j.dyepig.2017.10.018

Reference: DYPI 6316

To appear in: *Dyes and Pigments*

Received Date: 27 July 2017

Revised Date: 10 October 2017

Accepted Date: 12 October 2017

Please cite this article as: Hu W, Zhang X-F, Lu X, Lan S, Tian D, Li T, Wang L, Zhao S, Feng M, Zhang J, Modifying the *meso*-phenyl with electron donating amino groups strongly enhances BODIPY's ability as good singlet oxygen photosensitizer, *Dyes and Pigments* (2017), doi: 10.1016/j.dyepig.2017.10.018.

This is a PDF file of an unedited manuscript that has been accepted for publication. As a service to our customers we are providing this early version of the manuscript. The manuscript will undergo copyediting, typesetting, and review of the resulting proof before it is published in its final form. Please note that during the production process errors may be discovered which could affect the content, and all legal disclaimers that apply to the journal pertain.

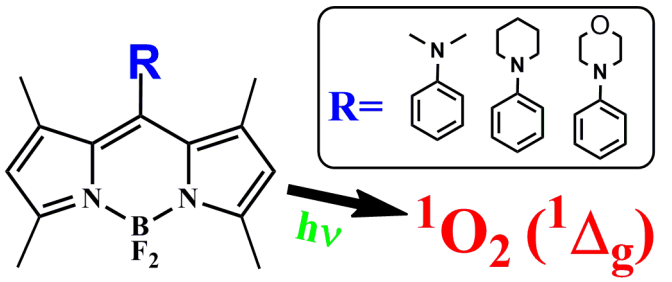

photoinduced charge transfer mechanism

ACCEPTED MANUSCRIPT

ACCEPTED MANUSCRIPT

Modifying the *meso*-phenyl with electron donating amino groups strongly enhances BODIPY's ability as good singlet oxygen photosensitizer

Wenbin Hu[a], Xian-Fu Zhang[b,*]

Xulin Lu[a], Shuai Lan[a], Dandan Tian[a], Tingting Li[a], Liangxia Wang[a], Siwen Zhao[a], Mingna Feng[a], Jing Zhang[a]

[a] Department of Chemical Engineering, Hebei Normal University of Science and Technology, Qinhuangdao, Hebei Province, China, 066004

[b] MPC Technologies, Hamilton, Ontario, Canada L8S 3H4

*Corresponding author

E-mail addresses: zhangxianfu@tsinghua.org.cn, zhangxf111@hotmail.com

ACCEPTED MANUSCRIPT

Abstract

We synthesized three 1,3,5,7-tetramethyl-BODIPY (**1a**, **2a**, **3a**) and three 3,5-dimethyl-BODIPY (**1b**, **2b**, **3b**) photosensitizers, in which the *meso* position was modified by different *para*-aminophenyl groups. The singlet oxygen generation and photophysical properties of the BODIPYs were studied by UV-vis absorption spectra, fluorescence emission spectra methods in various solvents. It was found that these BODIPY derivatives were environment-sensitive and fluorescent photosensitizers, which show high efficiency for generating singlet oxygen in medium polar environments but little photoactivity in polar and non polar solvents. In the mean time, they are highly fluorescent in nonpolar solvents but much less emissive in polar solvents, ICT emission occurs in medium polar solvents and correlated with singlet oxygen formation efficiency. The results are explained by PCT (photoinduced charge transfer) mechanism. The presence of the methyl groups at 1 and 7 positions disables the rotation of the phenyl ring, and therefore, the corresponding BODIPY **1a**, **2a**, and **3a** were characterized by significant higher singlet oxygen generation efficiency and fluorescence quantum yield than that of BODIPY **1b**, **2b**, and **3b**.

- Key words: BODIPY; singlet oxygen; fluorescence; charge transfer

ACCEPTED MANUSCRIPT

1. Introduction

Environment-sensitive fluorescent BODIPYs (boron dipyrromethene complexes) are attractive functional materials [1-9]. Their fluorescence properties are dependent on the hydrophobicity and polarity of the environment. These BODIPY molecules generally exhibit low fluorescence quantum yields in polar solvents, but became highly emissive in nonpolar solution [3-9]. Photoinduced electron transfer (PET) and photoinduced charge transfer (PCT) are widely acceptable mechanisms [3,10]. Take PCT for example, upon photoexcitation, a BODIPY molecule generates charge transfer state through the PCT mechanism, which makes the fluorescence of the fluorophore quenched. However, charge transfer state can be very active state. For example, by charge recombination intersystem crossing (CR ICT), charge transfer state could generate excited triplet state (T_1 state) [11-14], and T_1 state can lead to singlet oxygen formation and photochemical reactions [11,15-17]. The thought above drove us to explore whether electron donor substituted BODIPYs, such as amino-phenyl-BODIPY (electron donor-acceptor pair), could initiate T_1 and hence singlet oxygen ($^1\Delta_g$) formation which are key active species for photodynamic therapy of tumor.

8-(*para*-amino) phenyl substituted BODIPYs are well known PCT-based environment-sensitive fluorescence sensors [4,10,18,19], but have not been explored for singlet oxygen formation. In this study, we synthesized a series of PCT-based BODIPYs (**1a**, **2a** and **3a**) and the corresponding **1b**, **2b** and **3b** to study their singlet oxygen generation ability on the basis of our previous study [11, 15-17]. Because singlet oxygen plays the main role to damage tumor tissues in photodynamic therapy of tumor (PDT) [20], we hope this study may shed light on the novel PCT-based BODIPY photosensitizers for photodynamic therapy and open a new avenue for the development of more efficient BODIPY-type PDT agents.

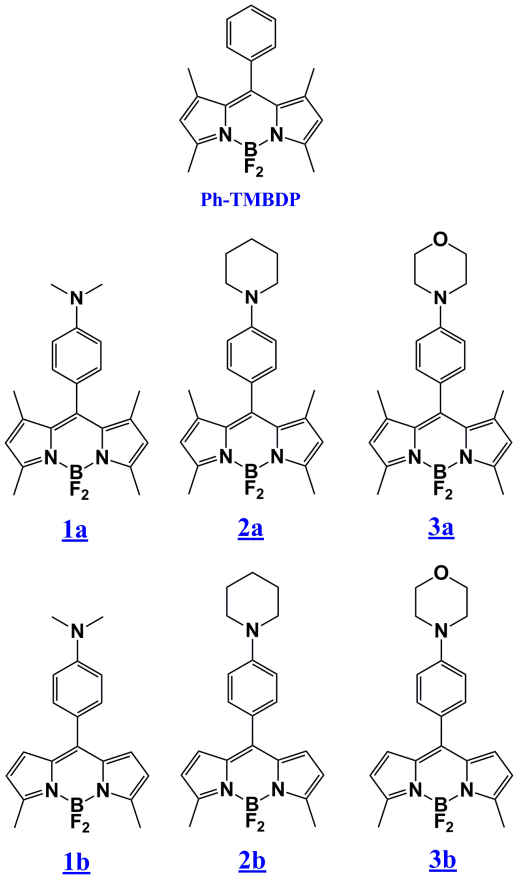

Fig. 1. Chemical structures of the studied BODIPYs

2. Experimental section

2.1. Reagents and apparatus.

All reagents and solvents were obtained from Sigma - Aldrich, Acros Organics, Merck or Fluka at the highest commercial grade and were used without further purification. Thin layer chromatography (TLC) was performed on Merck silica-gel 60 F254 plates to monitor reactions. Chromatographic purifications were performed on silica gel 60 (200-400 mesh) from Merck. ^{1}H NMR and ^{13}C NMR spectra were carried out on a Bruker dmx NMR spectrometer (600 MHz for ^{1}H NMR and 150 MHz for ^{13}C NMR) using chloroform-*d* as solvent. Chemical shifts were reported in

ppm. $CDCl_3$ (^1H: 7.26 ppm; ^{13}C: 77.16) was used as reference. High resolution APCI MS spectra were recorded on a LTQ Orbitrap XL APCI-TOF spectrometer.

2.2. *General procedure for the synthesis of 8-(para-amino substituted)phenyl BODIPYs* ***1a, 1b, 2a, 2b, 3a,*** *and* ***3b***

The synthesis follows the reported method in literature [3]. In an oven dried flask, 2,4-dimethylpyrrole (0.22 mL, 2.1 mmol) or 2-methylpyrrole (0.18 mL, 2.1 mmol) and the corresponding aldehyde (1.0 mmol) were dissolved in absolute dichloromethane (DCM, 20 mL). 50μL of TFA was added and the mixture was stirred at room temperature for 20 hours. When TLC revealed disappearance of the aldehyde, DDQ in dichloromethane (50 ml) was added to the solution, and stirred for 120 min. *N*,*N*-diisopropylethylamine (DIPEA, 5 mL) was added to the mixture and stirred at room temperature for 20 min. Then boron trifluoride etherate (3 mL) was added, and stirring was continued for 12 hours. The reaction mixture was washed twice with water and saturated NaCl, and was dried by anhydrous $MgSO_4$. The solvent was filtered and removed under vacuum. The crude compound was purified by silica gel flash chromatography using 30% DCM in petroleum ether to afford the pure sample.

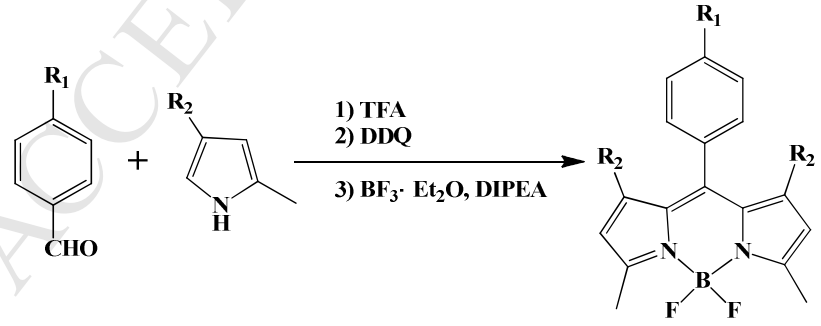

1a: R_1 = $-N(CH_3)_2$, $R_2 = CH_3$ **1b**: R_1 = $-N(CH_3)_2$, $R_2 = H$

2a: R_1= —N , $R_2 = CH_3$ **2b**: R_1= —N , $R_2 = H$

3a: R_1= —N O , $R_2 = CH_3$ **3b**: R_1= —N O , $R_2 = H$

Fig. 2. The synthetic path for the 8-(*para*-amino) phenyl substituted BODIPYs

10-(4-(dimethylamino)phenyl)-5,5-difluoro-1,3,7,9-tetramethyl-5H-dipyrrolo[1,2-c:2',1'-f][1,3,2]diazaborinin-4-ium-5-uide (**1a**). Yield: 12%. Orange crystals. ^{1}H NMR ($CDCl_3$, 600 MHz): δ 7.06 (d, J = 8.1 Hz, 2H), 6.77 (d, J = 8.2 Hz, 2H), 5.97 (s, 2H), 3.02 (s, 6H), 2.55 (s, 6H), 1.48 (s, 6H). ^{13}C NMR ($CDCl_3$, 150 MHz): δ 154.72, 150.63, 143.28, 143.22, 132.20, 128.72, 122.15, 120.85, 112.32, 40.37, 14.74, 14.60. ^{11}B NMR ($CDCl_3$, 200 MHz): δ 0.83 (t, 1B). HRMS (APCI) *m/z*: 348.2031 $[M-F]^+$ ($[M-F]^+$ calcd. 348.2047), *m/z*: 368.2089 $[M+H]^+$ ($[M+H]^+$ calcd. 368.2031)

10-(4-(dimethylamino)phenyl)-5,5-difluoro-3,7-dimethyl-5H-dipyrrolo[1,2-c:2',1'-f][1,3,2]diazaborinin-4-ium-5-uide (**1b**). Yield: 11%. Red crystals. ^{1}H NMR ($CDCl_3$, 600 MHz): δ 7.44 (d, J = 8.8 Hz, 2H), 6.84 (d, J = 4.0 Hz, 2H), 6.76 (d, J = 8.8 Hz, 2H), 6.26 (d, J = 4.0 Hz, 2H), 5.97 (s, 2H), 3.07 (s, 6H), 2.64 (s, 6H). ^{13}C NMR ($CDCl_3$, 150 MHz): δ155.62, 151.83, 143.87, 134.29, 132.42, 130.04, 121.90, 118.64, 111.30, 40.23, 14.84. ^{11}B NMR ($CDCl_3$, 200 MHz): δ 1.00 (t, 1B). HRMS (APCI) *m/z*: 320.1721 $[M-F]^+$ ($[M-F]^+$ calcd. 320.1734), *m/z*: 340.1780 $[M+H]^+$ ($[M+H]^+$ calcd. 340.1718)

5,5-difluoro-1,3,7,9-tetramethyl-10-(4-(piperidin-1-yl)phenyl)-5H-dipyrrolo[1,2-c:2',1'-f][1,3,2]diazaborinin-4-ium-5-uide (**2a**). Yield: 13%. Orange crystals. ^{1}H NMR ($CDCl_3$, 600 MHz): δ 7.08 (d, J = 8.5 Hz, 2H), 7.01 (d, J = 8.5 Hz, 2H), 5.96 (s, 2H), 3.23 (t, J = 7.2, 6.3 Hz, 4H), 2.54 (s, 6H), 1.74 (m, J = 5.8 Hz, 4H), 1.61 (m, J = 6.0 Hz, 4H), 1.46 (s, 6H). ^{13}C NMR ($CDCl_3$, 150 MHz): δ154.90, 152.46, 143.28, 142.75, 132.01, 128.64, 124.82, 120.93, 116.28, 50.12, 25.66, 24.25, 14.69, 14.61. ^{11}B NMR ($CDCl_3$, 200 MHz): δ 0.81 (t, 1B). HRMS (APCI) *m/z*: 388.2342 $[M-F]^+$ ($[M-F]^+$ calcd. 388.2360), *m/z*: 408.2401 $[M+H]^+$ ($[M+H]^+$ calcd. 408.2344)

5,5-difluoro-3,7-dimethyl-10-(4-(piperidin-1-yl)phenyl)-5H-dipyrrolo[1,2-c:2',1'-f][1,3,2]diazaborinin-4-ium-5-uide (**2b**). Yield: 11%. Red crystals. ^{1}H NMR ($CDCl_3$,

600 MHz): δ 7.42 (d, J = 8.8 Hz, 2H), 6.96 (d, J = 8.8 Hz, 2H), 6.82 (d, J = 4.0 Hz, 2H), 6.26 (d, J = 4.1 Hz, 2H), 5.96 (s, 2H), 3.32 (t, 4H), 2.64 (s, 6H), 1.72 (p, J = 5.6 Hz, 4H), 1.65 (p, J = 5.6 Hz, 4H). ^{13}C NMR ($CDCl_3$, 150 MHz): δ 155.98, 153.08, 143.50, 134.34, 132.23, 130.11, 123.72, 118.77, 114.40, 49.22, 25.57, 24.33, 14.87. ^{11}B NMR ($CDCl_3$, 200 MHz): δ 0.99 (t, 1B). HRMS (APCI) *m/z*: 360.2034 $[M-F]^+$ ($[M-F]^+$ calcd. 360.2047), *m/z*: $[M+H]^+$ 380.2094 ($[M+H]^+$ calcd. 380.2031)

5,5-difluoro-1,3,7,9-tetramethyl-10-(4-morpholinophenyl)-5H-dipyrrolo[1,2-c:2',1'-f][1,3,2]diazaborinin-4-ium-5-uide (**3a**). Yield: 13%. Orange crystals. ^{1}H NMR ($CDCl_3$, 600 MHz): δ 7.12 (d, J = 8.1 Hz, 2H), 6.99 (d, J = 8.1 Hz, 2H), 5.97 (s, 2H), 3.90 (t, J = 4.7 Hz, 4H), 3.23 (t, J = 4.8 Hz, 4H), 2.54 (s, 6H), 1.45 (s, 6H). ^{13}C NMR ($CDCl_3$, 150 MHz): δ155.09, 151.59, 143.19, 142.25, 131.92, 128.86, 125.86, 121.03, 115.54, 66.78, 48.79, 14.69, 14.62. ^{11}B NMR ($CDCl_3$, 200 MHz): δ 0.80 (t, 1B). HRMS (APCI) *m/z*: $[M-F]^+$ 390.2137 ($[M-F]^+$ calcd. 390.2153), *m/z*: $[M+H]^+$ 410.2195 ($[M+H]^+$ calcd. 410.2137)

5,5-difluoro-3,7-dimethyl-10-(4-morpholinophenyl)-5H-dipyrrolo[1,2-c:2',1'-f][1,3,2]diazaborinin-4-ium-5-uide (**3b**). Yield: 11%. Red crystals. ^{1}H NMR ($CDCl_3$, 600 MHz): δ 7.44 (d, J = 8.3 Hz, 2H), 6.96 (d, J = 8.0 Hz, 2H), 6.79 (d, J = 4.1 Hz, 2H), 6.27 (d, J = 4.1 Hz, 2H), 3.89 (t, J = 4.9 Hz, 4H), 3.29 (s, 4H), 2.64 (s, 6H). ^{13}C NMR ($CDCl_3$, 150 MHz): δ156.47, 152.51, 143.01, 134.38, 132.07, 130.15, 125.05, 118.99, 114.18, 66.75, 48.16, 14.90. ^{11}B NMR ($CDCl_3$, 200 MHz): δ 0.98 (t, 1B). HRMS (APCI) *m/z*: $[M-F]^+$ 362.1826 ($[M-F]^+$ calcd. 362.1840), *m/z*: $[M+H]^+$ 382.1885 ($[M+H]^+$ calcd. 382.1824)

2.3. Photophysical measurements

The procedure for fluorescence and singlet oxygen measurements are similar to our previous reports [11, 15-17].

2.3.1. Absorption measurements.

Ground-state UV−vis absorption spectra were obtained on a Vary 8454 spectrometer from Agilent Technologies which was connected to a deuterium and halogen lamp by Optical fiber using 1 cm matched quartz cuvettes at 20 ºC.

2.3.2. Fluorescence measurements.

The measurements on fluorescence spectra, fluorescence quantum yields, and the fluorescence lifetimes were performed at 20 ºC. Steady state fluorescence studies were performed with a FLS920 Fluorescence Spectrometer from Edinburgh Instruments. The slit width was 0.5 nm for both excitation and emission. All spectra were corrected for the sensitivity of the photomultiplier tube.

The fluorescence quantum yield (Φ_f) of each BODIPY derivative was obtained by comparing the emission spectra of the test sample with that of a 10 mM PBS buffer solution of 2,4,5,7-tetrabromo fluorescein excited at 475 nm, whose fluorescence quantum yield is 0.24 according to the literature [21]. The sample and reference solutions were prepared with the same absorbance (~0.090) at 475 nm. The fluorescence quantum yield (Φ_f) was obtained according to the following equation:

$$\Phi_f = \Phi_f^0 \cdot \frac{F_s}{F_0} \cdot \frac{A_0}{A_s} \cdot \frac{n_s^2}{n_0^2} \qquad (1)$$

where F denotes the integrated fluorescence intensity, s represents the sample, the

subscript 0 stands for the reference compound, n denotes the refractive index of the solvent, and A denotes the absorbance at the excitation wavelength. All solutions were air saturated, and all spectra were recorded at 20 °C.

2.3.3. Singlet oxygen quantum yield

Singlet oxygen quantum yield (Φ_{Δ}) determinations were measured by the chemical trapping method [22]. The solvents were air saturated. The absorbance of a solution of the BODIPYs is ca. 1.0 at 509 nm (close to the absorption maximum of the BODIPY). The solution was irradiated at 509 nm by a LED light source. The concentration of DPBF was decreased to 3×10^{-5} M in order to avoid the chain reactions induced by DPBF in the presence of singlet oxygen. The degradation of DPBF was monitored by UV−vis absorption spectra at 410 nm. The Φ_{Δ} values were calculated with the following equation:

$$\Phi_{\Delta} = \Phi_{\Delta}^{\mathrm{ref}} \cdot \frac{k}{k_{\mathrm{ref}}} \cdot \frac{I_{\mathrm{a}}^{\mathrm{ref}}}{I_{\mathrm{a}}} \qquad (2)$$

$\Phi_{\Delta}^{\mathrm{ref}}$ denotes the singlet oxygen quantum yield of solvent-independent standard 8-methylthio-2,6-diiodoBODIPY ($\Phi_{\Delta}^{\mathrm{ref}} \approx 0.80$) [23]. k and k_{ref} denote the photobleaching rate constants of DPBF in the presence of samples and reference compound, respectively. I_{a} and $I_{\mathrm{a}}^{\mathrm{ref}}$ denote the light absorption rates at 509 nm of the samples and reference compound. Their ratio can be calculated with the following equation:

$$\frac{I_a^{ref}}{Ia} = \frac{1-10^{-A_{509}^{ref}}}{1-10^{-A_{509}}} \qquad (3)$$

In which A_{509} and A_{509}^{ref} denote the absorbance of at 509 nm of the BODIPY and reference compound.

2.4. Laser flash photolysis for excited triplet state

Transient absorption spectra were recorded in THF solution with an Edinburgh LP920 laser flash photolysis system. An OPO laser (500 nm and 4 ns FWHM, 2 mJ) was used as excitation source. The analyzing light was from a pulsed xenon lamp. The laser and analyzing light beams perpendicularly passed through a quartz cell with an optical path length of 1 cm. The signal was displayed and recorded on a Tektronix TDS 3012B oscilloscope and an R928B detector. The laser energy incident at the sample was attenuated to ca. 2 mJ per pulse. Time profiles at a series of wavelengths from which point by-point spectra were assembled were recorded with the aid of a Pc controlled kinetic absorption spectrometer. The concentrations of the target compounds were typically 20 μM providing A_{500} = 1.0 in a 10 mm cuvettes.

2.5. Quantum chemical computation

The calculations were carried out using density functional theory (DFT) method as implemented in the Gaussian 09 package. The B3LYP exchange-correlation functional was chosen together with a 6-31G(d) basis set for structural optimization. The solvent effect was modeled using the Polarizable Continuum Model (CPCM) method. In all the cases frequency analysis was made after geometry optimization to ensure the convergence to an energy minimum.

3. Results and discussion

The six compounds were prepared by the well established synthetic procedure for BODIPYs. NMR and HRMS data are well consistent with the structures as given in the experimental section. These BODIPY derivatives are well soluble in both non polar and polar solvents, such as benzene, n-hexane, toluene, DCM, chloroform, ethyl acetate, THF, acetone, acetonitrile, DMF, DMSO, ethanol and methanol and so on. Therefore seven solvents (*n*-hexane, ethyl acetate, THF, pinacolone, acetone, methanol and acetonitrile) ranging from nonpolar, medium polar and high polar were selected to measure their singlet oxygen generation ability.

3.1. Ground state UV-Vis absorption

Table 1 and Figure 3 show the UV−vis absorption properties of the BODIPY derivatives in several solvents. Their spectra showed the typical absorption bands of BODIPY chromophore, in which a strong absorption band is located around 500 nm with a shoulder at 480 nm. The spectral shape of **1a**, **2a**, and **3a** are only slightly affected by either *para*-substitutents of the phenyl or the solvents used. With the increase in solvent polarity, the shape of the absorption spectra is slightly broadened due to the weak ground state charge transfer interaction. The peak maximum values are blue shifted by only 4 nm, which is also in line with the general behavior of BODIPYs. Therefore, in the ground-state configuration there are two independent π systems within each compound **1a**, **2a**, and **3a**: the phenyl group and the perpendicular BODIPY core, which have little electronic coupling and form a donor−acceptor pair. The BODIPY core is the fluorophore and acts as an electron acceptor. The attached amino phenyl group acts as an electron donor. A detailed inspection of the spectra of **1b**, **2b**, and **3b** shows that a weak shoulder at 550 nm exists, which became more obvious when the polarity of solvents is increased. This indicates that the weak band at 550 nm is due to charge transfer [5]. Compared to **1a**,

2a, and **3a**, the two methyls at 1 and 7 positions of BODIPY are absent in compound **1b**, **2b**, and **3b**, which makes the phenyl and the attached BODIPY core are not perpendicular but have a dihedral angle ca. 60^{o}. This angle increases the electron cloud overlapping between the amino phenyl and the BODIPY core, and makes the charge transfer from the amino phenyl to the attached BODIPY core easier.

The absorption maximum of **1b**, **2b**, **3b** are 6-10 nm larger than that of **1a**, **2a**, **3a**. This is due to the inductive effect +I of the methyl groups, which raise up the energy of the LUMO state with regard to that of the HOMO. This results in a slight increase in the energy gap between both states, and therefore causes the hypsochromic shifts [13].

Table 1. The photophysical characteristics of BODIPY **1**-**3** in several solvents

	solvent	Φ_f	Φ_Δ	λ_{max}^{abs} (nm)	λ_{max}^{em} (nm)	$\Delta\lambda$ (nm)
	n-hexane	0.441	0.102	500	511	11
	EtOAc	0.011	0.412	498	510	12
	THF	0.014	0.623	499	513	14
BODIPY **1a**	**Pinacolone**	0.015	0.490	496	511	15
	Acetone	0.009	0.114	496	510	14
	MeOH	0.003	0.073	492	511	19
	CH_3CN	0.005	0.062	496	508	12
	n-hexane	0.376	0.230	507	519	12
	EtOAc	0.013	0.171	504	513	9
BODIPY **1b**	**THF**	0.011	0.321	506	517	11
	Pinacolone	0.024	0.439	505	512	7
	Acetone	0.006	0.087	504	515	11

	MeOH	0.030	0.019	503	511	8
	CH_3CN	0.008	0.052	503	511	8
	n-hexane	0.384	0.058	500	511	11
	EtOAc	0.006	0.511	498	515	17
	THF	0.008	0.612	499	515	16
BODIPY **2a**	**Pinacolone**	0.024	0.644	496	516	20
	Acetone	0.002	0.145	495	515	20
	MeOH	0.010	0.037	497	514	17
	CH_3CN	0.005	0.083	496	511	15
	n-hexane	0.341	0.258	506	520	14
	EtOAc	0.005	0.220	505	518	13
	THF	0.008	0.401	504	514	10
BODIPY **2b**	**Pinacolone**	0.004	0.457	506	523	17
	Acetone	0.002	0.099	506	517	11
	MeOH	0.003	0.046	504	518	14
	CH_3CN	0.002	0.057	504	519	15
	n-hexane	0.450	0.120	498	511	13
	EtOAc	0.029	0.676	498	517	19
	THF	0.011	0.535	500	514	14
BODIPY **3a**	**Pinacolone**	0.063	0.588	495	520	25
	Acetone	0.001	0.192	490	516	26
	MeOH	0.002	0.038	494	514	20
	CH_3CN	0.001	0.083	496	511	15
BODIPY **3b**	**n-hexane**	0.388	0.225	508	520	12

EtOAc	0.008	0.290	506	520	14
THF	0.004	0.338	507	528	21
Pinacolone	0.002	0.281	506	530	24
Acetone	0.002	0.100	505	517	12
MeOH	0.005	0.008	505	521	16
CH_3CN	0.020	0.033	505	534	29

Φ_f: the fluorescence quantum yield, Φ_Δ: the quantum yield for singlet oxygen formation, λ_{max}^{abs}: the UV−vis absorption maximum, λ_{max}^{em}: the fluorescence emission maximum, $\Delta\lambda$: the Stokes shift.

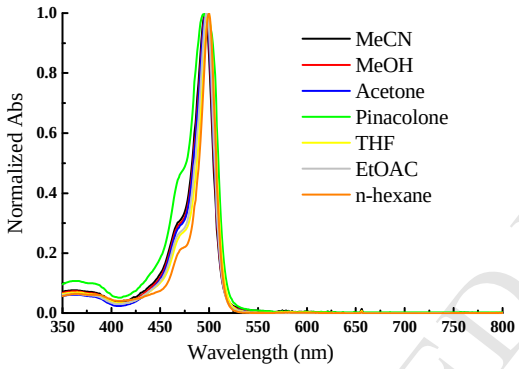

1a

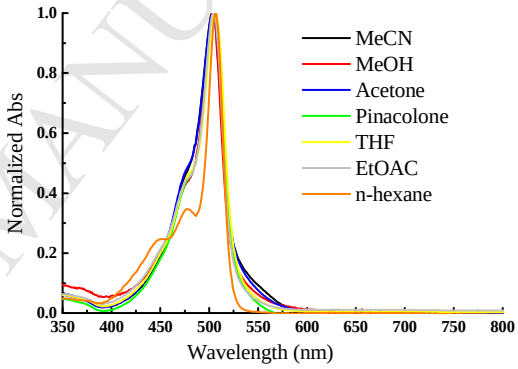

1b

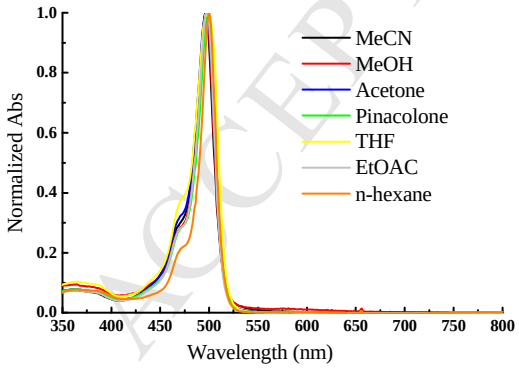

2a

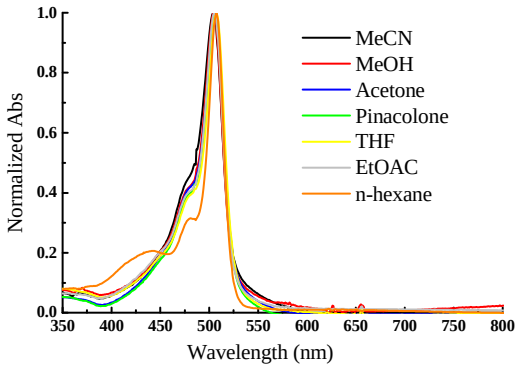

2b

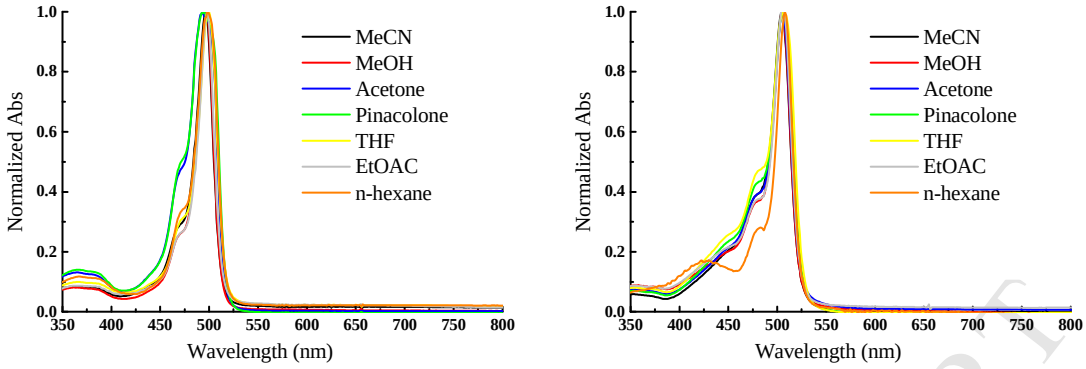

Fig. 3. Normalized absorption spectra of **1** - **3** in different solvents.

3.2. Fluorescence studies

The fluorescence emission of the BODIPYs is strongly solvent dependent. With the increase in solvent polarity, new emission bands appear for all the amino phenyl-BODIPYs, but not for Ph-TMBDP. The new band is broad and structureless, which shows the typical feature of charge transfer emission (CT emission). Apparently the presence of amino groups is responsible for the charge transfer. The CT band intensity is **1a** < **2a**< **3a** and **1b** < **2b**< **3b,** which is consistent with the ranking of the electron donating ability of the amino groups attached on the phenyl.

The fluorescence quantum yield (Φ_f) values of Ph-TMBDP are 0.57±0.04 in different solvents, which is little affected by the solvent polarity. The Φ_f of any amino phenyl substituted BODIPY (Table 1) in any solvent is always smaller than that of Ph-TMBDP, in particular in polar solvents. This indicates that amino phenyl unit quenches the S_1 state of the attached TMBDP unit, due to charge transfer process from S_1 state (^{1}BODIPY-Donor → BODIPY$^{[\delta-]}$-Donor$^{[\delta+]}$) [24]. In addition, Φ_f of the BODIPYs is very dependent on the solvent polarity. The values of Φ_f decrease with increasing solvent polarity from *n*-hexane to acetonitrile. To explain the solvent effects on the phenomenon above, we can view the BODIPYs as electron donor/acceptor pairs. The intramolecular charge transfer (ICT) occurs upon light

irradiation and leads to the formation of the excited state with a large dipole moment. The intramolecular charge transfer (ICT) is favored by high polar solvents [25-27]. Therefore, increasing the solvent polarity leads to a faster decay of the S_1 and a lower fluorescence quantum yield. In medium polar solvents, the intramolecular charge transfer causes a red-shifted new emission band [13]. In highly polar solvents, the red-shifted emission is so weak that it can hardly be detected due to the fast charge recombination of the ICT state [5,13]. **2a** and **3a** showed the stronger ICT emission, probably because the six member ring (or the γ atoms of the six member ring) may stabilize the positive charge and create additional charge transfer [28].

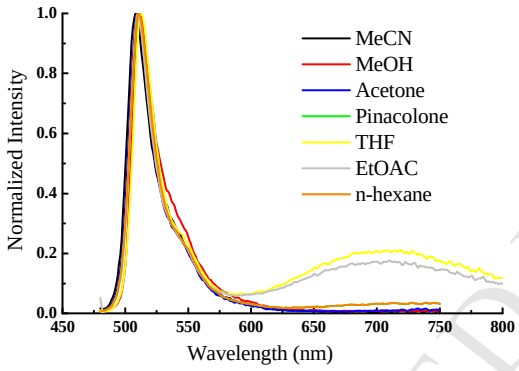

1a

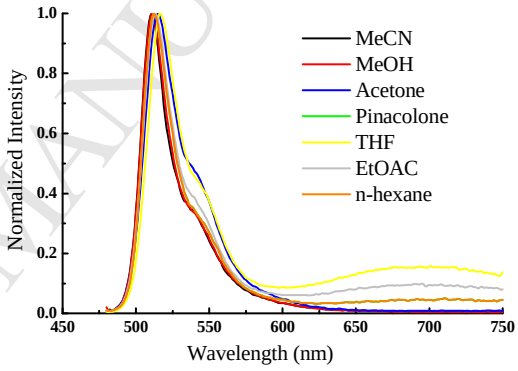

1b

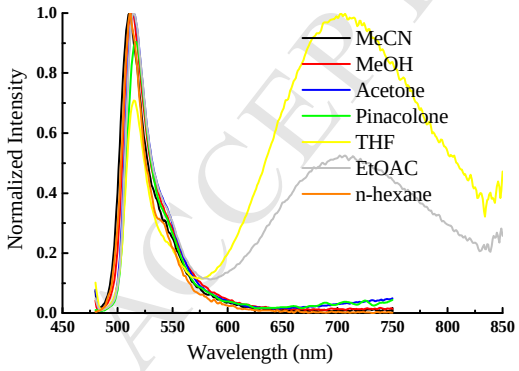

2a

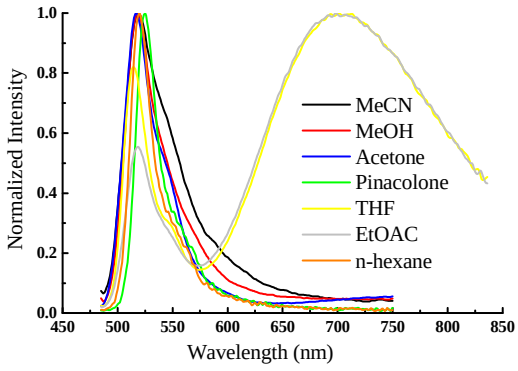

2b

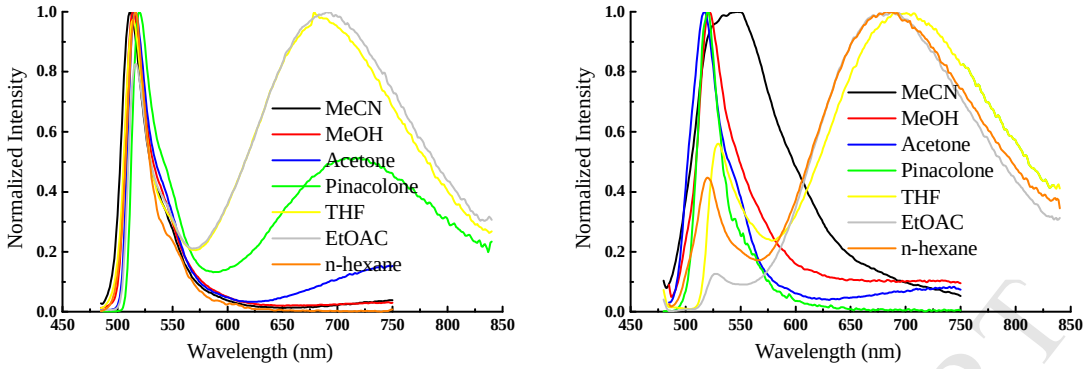

3a **3b**

Fig. 4. Normalized fluorescence emission spectra of the BODIPYs in different solvents with excitation at 475 nm

The fluorescence quantum yields for **1a** - **3a** were greater than those for the corresponding **1b** - **3b**. Because **1b** - **3b** are not substituted by methyl groups at the 1 and 7 positions, the phenyl ring has greater freedom of rotation, which increases the amount of energy loss via non radiative decay.

The presence of PCT within amino phenyl-TMBDP is also supported by the HOMO/LUMO distribution of the compounds (Fig. 5). For example, the LUMO of **1a** is located on the TMBDP moiety, while its HOMO is on the dimethylamino phenyl unit. This means that upon photoexcitation, electron charge will be relocated from one unit to another attached moiety, i.e. PCT occurs. For Ph-TMBDP, however, both LUMO and HOMO are located on the TMBDP moiety, no PCT is possible. This result shows that the dimethylamino substitution on the phenyl unit has a remarkable positive effect on PCT, since it increases the electron donating ability of the phenyl and makes PCT more likely, and causes the fluorescence quenching of TMBDP and the enhancement on T_1 and singlet oxygen formation.

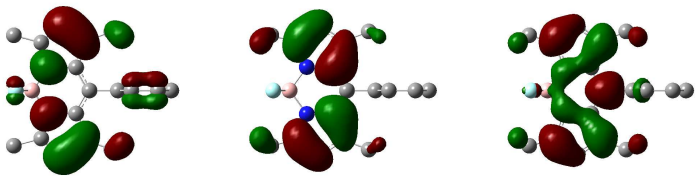

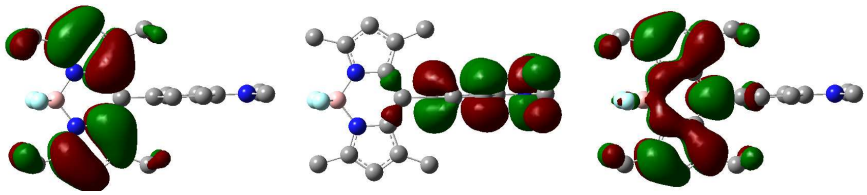

Fig. 5. Top: the HOMO-1, HOMO, and LUMO of compound **Ph-TMBDP** in MeCN. Bottom: the HOMO-1, HOMO, and LUMO of compound **1a** in MeCN.

3.3. Singlet oxygen formation

The singlet oxygen generation capacity of the BODIPYs was measured in several organic solvents. 1,3-diphenyl-iso-benzofuran (DPBF) was used since it is the widely known quantitative and specific singlet oxygen trapper for the determination of the formation quantum yield of singlet oxygen. The light irradiations at 510 nm were used since it is absorbed by BODIPYs but not by DPBF. The absorption band of DPBF at 410 nm was gradually reduced with the light irradiation up to 30 minutes in the presence of a BODIPY, but BODIPYs did not show any absorption change (Fig. 6). The absorbance change of DPBF is linearly correlated to time t (Fig. 7). In the absence of either the BODIPY or light, no DPBF degradation occurred, indicating that the BODIPYs indeed produced singlet oxygen and caused the oxidation of DPBF.

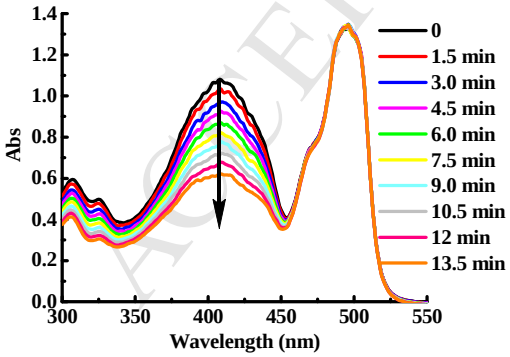

Fig. 6. The change of absorption spectrum of DPBF in the presence of **3a** in EtOAc with irradiation at 510 nm

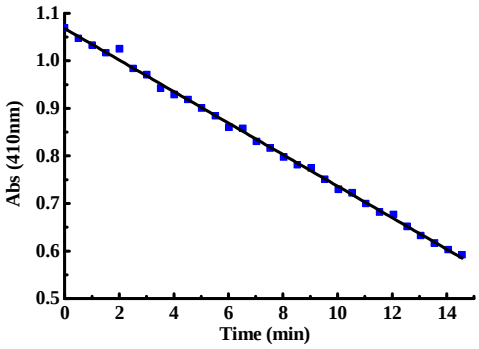

Fig. 7. The plot of DPBF absorbance at 410 nm against time and the fitting

The singlet oxygen formation quantum yields (Φ_Δ) of the Ph-TMBDP are 0.040±0.02 in the solvents studied. In contrast, the Φ_Δ of any amino phenyl substituted BODIPY (Table 1) is always much higher than that of Ph-TMBDP in polar solvents EtOAc, THF, pinacolone and acetone (Φ_Δ can be as high as close to 0.70). This indicates that the amino presence significantly enhances the formation of singlet oxygen which is coincident with the fluorescence quenching due to charge transfer process from S_1 state (^{1}BODIPY-Donor → BODIPY$^{[\delta-]}$-Donor$^{[\delta+]}$). We then conclude that the charge transfer causes the T_1 formation (BODIPY$^{[\delta-]}$-Donor$^{[\delta+]}$ → ^{3}BODIPY-Donor), since T_1 is the precursor of singlet oxygen (^{3}BODIPY-Donor + O_2 → BODIPY-Donor + $^1O_2$).

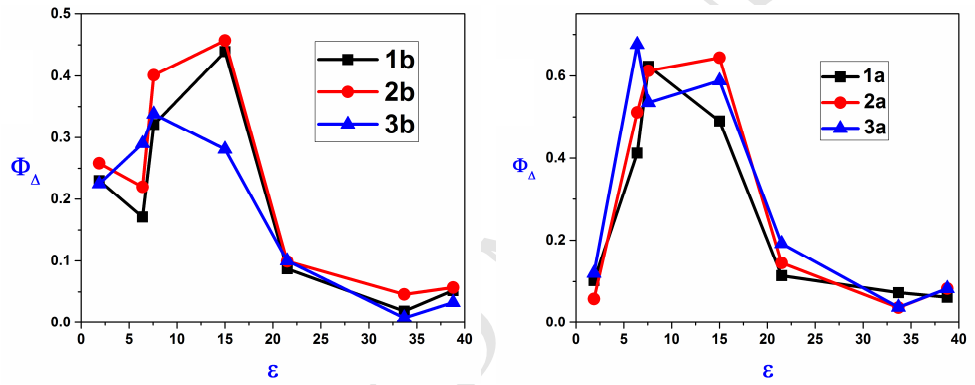

Fig. 8. The dependence of Φ_Δ on the solvent polarity (dielectric constant ε).

Fig. 8 shows the dependence of Φ_Δ on solvent polarity (represented by the dielectric constant ε). The highest Φ_Δ was obtained when ε is about 15. Fig. 8 also tells the effect of the electron-donating ability of the amino phenyl substituent on the quantum yields. Φ_Δ of **2b** is slightly higher than that of **1b**, while Φ_Δ of **1b** is higher than that of **3b**. Φ_Δ of **2a** in most cases is higher than that of **3a** and **1a**. The performance of **2b** and **2a** indicates that the substitutents with medium electron donating ability are better. Also noted is that the Φ_Δ of BODIPY **1b**-**3b** are lower than those of BODIPY **1a**-**3a**. This is due to the free rotation of the phenyl units of **1b**-**3b** (because of the absence of 1,7-dimethyl compared to that in **1a**-**3a**), which causes

more S_1 states going back to S_0 by heat releasing rather than charge transfer.

For each compound, observing Φ_Δ values in Table 1 and ICT emission intensity (I_{ICT}) of Fig. 4 in different solvents, it is clear that the higher the I_{ICT} is, the higher the Φ_Δ value is. This close relationship also indicates that the singlet oxygen generation ability depends on the ICT state. In other words, triplet state T_1 is from ICT state (process 1-6 below), since singlet oxygen comes from energy transfer of T_1 state.

1. BODIPY-Donor + hν → ^{1}BODIPY-Donor, light absorption to form excited state.
2. ^{1}BODIPY-Donor → BODIPY$^{[\delta-]}$-Donor$^{[\delta+]}$, ICT process.
3. BODIPY$^{[\delta-]}$-Donor$^{[\delta+]}$ → ^{3}BODIPY-Donor, charge recombination (CR) to form T_1 state.
4. BODIPY$^{[\delta-]}$-Donor$^{[\delta+]}$ → BODIPY-Donor+ heat, CR to form ground state.
5. BODIPY$^{[\delta-]}$-Donor$^{[\delta+]}$ → BODIPY-Donor+ hν', CR to luminescence (ICT emission).
6. ^{3}BODIPY-Donor + O_2 → BODIPY-Donor + $^1O_2$, energy transfer to from singlet oxygen.
7. $^1O_2$ + DPBF → decomposed product.

Based on the mechanism above, we can explain why the emission spectra for EtOAc and THF are very different from those in other solvents (Fig 4 in which I_{ICT} is higher for THF and EtOAc). Increasing solvent polarity enhances both process 2 and process 4, but enhancing process 2 makes more BODIPY$^{[\delta-]}$-Donor$^{[\delta+]}$ and so ICT emission should becomes higher. However, enhancing process 4 consumes more BODIPY$^{[\delta-]}$-Donor$^{[\delta+]}$ by heat releasing, so ICT emission becomes lower. When the solvent polarity is too high, process 4 (heat releasing) will dominate, ICT emission and singlet oxygen formation become very weak. On the other hand, if the solvent polarity is too low, process 2 will be absent and no ICT state is formed, therefore no ICT emission and the associated triplet state formation. EtOAc and THF have medium polarity, PCT process 2 is fast while heat releasing process is still slow, so that ICT emission and the associated triplet state formation yield are high.

Laser flash photolysis (LFP) technique was used to examine the formation of

excited triplet state with excitation at 500 nm (4 ns pulse) in air saturated THF solutions. The transient absorption spectra (TAS) and the triplet decay curves are shown in Fig. 9. The positive absorption bands were observed at about 430 nm for **1a** and **2a**. No significant signal was detected for Ph-TMBDP. The band shape and positions are similar to the reported T_1-T_n absorption of other BODIPY analogues [16, 17]. The lifetime is 0.37 and 0.43 μs in air saturated THF for **1a** and **2a** respectively, but it became much longer, i.e. 36 and 39 μs in argon saturated THF respectively. These results show that excited triplet state was indeed formed for the amino phenyl substituted BODIPYs.

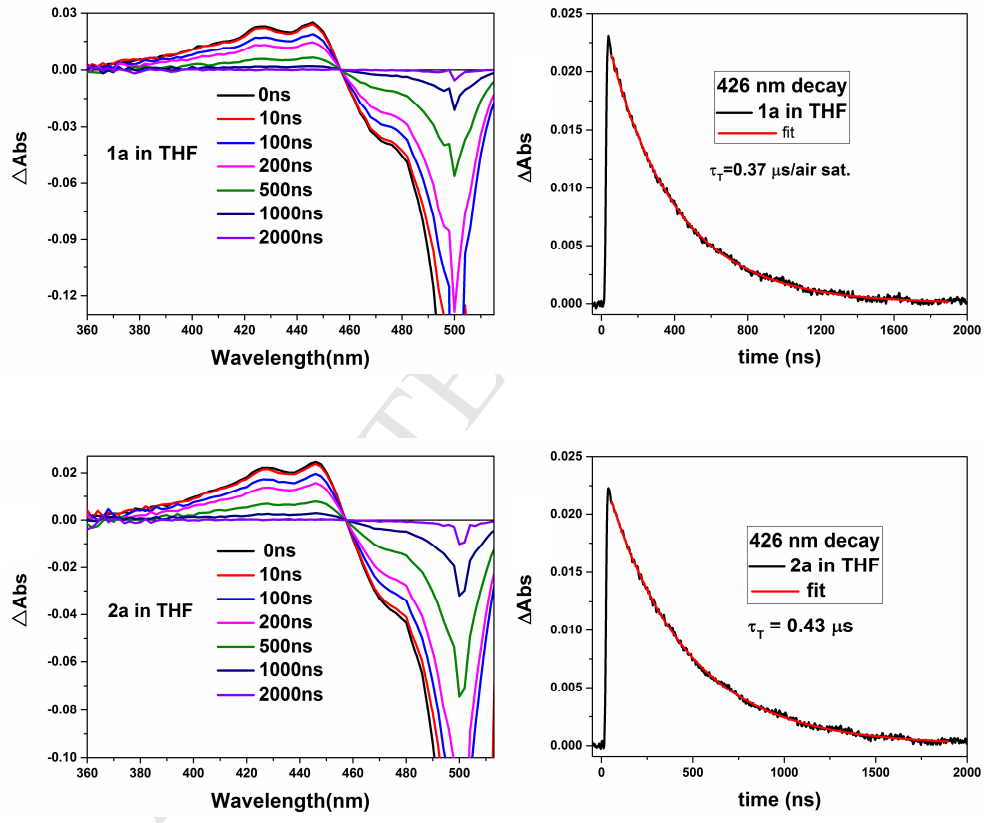

Fig. 9. μs scaled transient absorption spectra (Left) and the decay of positive transient absorbance (Right) in air saturated THF solution (20 μM), excitation wavelength is 500 nm (2 mJ, 4 ns OPO pulsed laser). Top: **1a**, Bottom: **2a**.

The photophysical processes proposed above can be shown in Fig. 10. Upon photoexcitation, 8-(*para*-amino) phenyl substituted BODIPYs generate charge transfer state, and charge transfer state forms excited triplet state (T_1 state), ICT emission and ground state by charge recombination (backward electron transfer). T_1 state causes the energy transfer to molecular oxygen to form singlet oxygen.

Table 1 summarized the Φ_Δ results. Apparently the BODIPYs showed efficient generation of singlet oxygen in medium polar environments but little photo active in polar and non polar solvents. In non polar solvent, no ICT state is formed, therefore no T_1 state and singlet oxygen formation. In high polar solvent, process 4 (heat releasing) is very fast and predominant, so that process 3 (T_1 formation) and 5 (ICT emission) are not competent.

BODIPY **1a**, **2a**, and **3a** exhibited higher singlet oxygen generation efficiency than the corresponding **1b**, **2b**, and **3b**, since the presence of the methyl groups at the 1, and 7 positions of the s-indacene ring causes the large steric hindrance for the rotation of the phenyl group, and reduces heat releasing.

Based on the mechanism above, the experimental results of the studied BODIPYs could be explained below.

1. In non polar solvent, the energy of S_1 is mainly released as light emission.

2. With the increase in solvent polarity, the intramolecular charge transfer becomes more and more favored, and the number of molecules in charge transfer state increases.

3. In medium polar solvents, charge transfer state produces excited triplet state, which leads to the formation of singlet oxygen. DPBF is then decomposed by singlet oxygen.

4. In high polar solvents, the energy of charge transfer state is mainly released as heat: BODIPY$^{[\delta-]}$-Donor$^{[\delta+]}$ $\rightarrow$ BODIPY-Donor+ heat. Process 3 (T_1 formation) and 5 (ICT emission) are not competent and negligible.

5. The methyl groups at the 1 and 7 positions of the s-indacene ring hinders the rotation of the phenyl rings and results in significantly higher fluorescence quantum yields and the quantum yields of singlet oxygen formation.

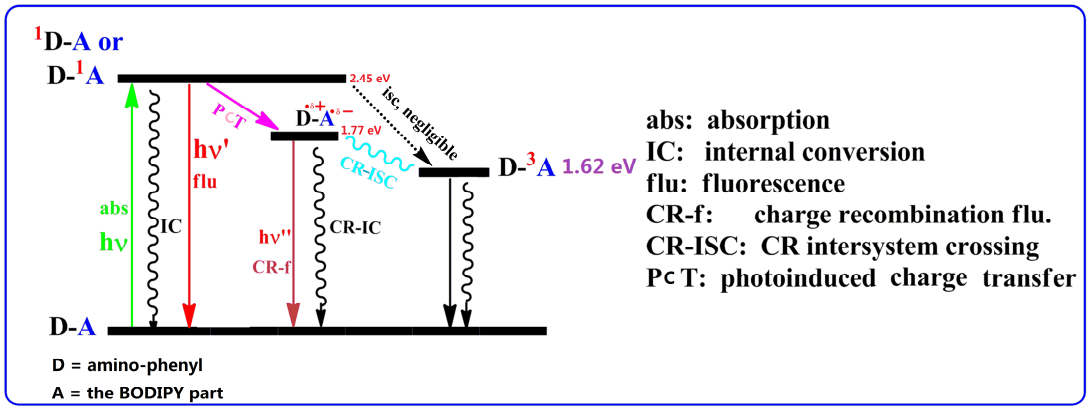

Fig. 10. Photophysics and energy level for T_1 formation by PCT mechanism.

4. Conclusions

We synthesized six 8-*para*-amino phenyl substituted BODIPY photosensitizers. These BODIPYs showed the efficient generation of singlet oxygen in medium polar environments. Φ_f and Φ_Δ of the BODIPYs are related to both the structure of the donor moiety and solvent polarity due to PCT (photoinduced charge transfer) mechanism. Incorporating methyl groups at the 1 and 7 positions of the BODIPY core decreases the degree of rotational freedom, which leads to the increase in the quantum yield for both fluorescence and singlet oxygen formation, while Φ_f is decreased with the increase in solvent polarity. These novel photosensitizers based on PCT mechanism indicate their potential application in photodynamic therapy of cancer.

Acknowledgements

This work is supported by the Natural Science Foundation of Hebei Province (Contract B2016407084 and B2014407080), Youth Talent Program of Hebei High School (Contract BJ2017028), and Technology Foundation for Selected Overseas Chinese Scholar of Hebei Province (Contract C2015003046). We also thank the financial support from Hebei Provincial Hundred Talents Plan (Contract E2013100005) and HBUST (Contract CXTD2012-05).

References

[1] Zhao J, Xu K, Yang W, Wang Z, Zhong F. Chem Soc Rev. 2015;44(24):8904-39.

[2] Zhao J, Huang L, Cui X, Li S, Wu H. J. Mater. Chem. B, 2015; 3:9194-9211.

[3] H. Sunahara,Y. Urano, H. Kojima, T. Nagano, J. Am. Chem. Soc., 2007, 129, 5597-5604.

[4] M. Baruah , W. Qin , N. Basarić , W. M. De Borggraeve , N. Boens, J. Org. Chem., 2005, 70, 4152-4157.

[5] A. Filarowski, M. Kluba, K. Cieslik-Boczula, A. Koll, A. Kochel, L. Pandey, W. M. De Borggraeve, M. Van der Auweraer, J. Catalanc, N. Boens, Photochem. Photobiol. Sci., 2010, 2010, 996-1008.

[6] P. Bukowska, J. Piechowska, R. Loska, Dyes and Pigments, 2017, 137, 312-321.

[7] R. I. Roacho, A. Metta-Magaña, M. M. Portillo, E. Peña-Cabrera, K. H. Pannell, J. Org. Chem., 2013, 78, 4245−4250.

[8] C. Yu, Q. Wu, Z. Tian, T. Li, E. Hao, L. Jiao, J. Porphyrins Phthalocyanines, 2016, 2016, 1–15.

[9] E. V. Antina, N. A. Bumagina, A. I. V'yugin, A. V. Solomonov, Dyes and Pigments, 2017, 136, 368-381.

[10] W. Qin, M. Baruah, M. Van der Auweraer, F. C. De Schryver, N. Boens, J. Phys. Chem. A, 2005, 109, 7371-7384.

[11] X.-F. Zhang, N. Feng, Chem. Asian J., 2017, 12, 2447-2456.

[12] S. H. Park, A. Roy, S. Beaupré, S. Cho, N. Coates, J. S. Moon, D. Moses, M. Leclerc, K. Lee, A. J. Heege, Nature Photon. 2009, 3, 297-302.

[13] P. Janssen, S. H.W. Wouters, M. Cox, B. Koopmans, Org. Electron. 2014, 15, 743–750.

[14] W. Chang, D. N. Congreve, E. Hontz, M. E. Bahlke, D. P. McMahon, S. Reineke, T. C. Wu, V. Bulović, T. Van Voorhis, M. A. Baldo, Nat. Commun., 2015, 6, 6415.

[15] X.-F. Zhang, X. Yang, B. Xu, Phys. Chem. Chem. Phys. 2017, 19(36), 24792-804.

[16] X.-F. Zhang, Dyes and Pigments. 2017,146, 491-501.

[17] X.-F. Zhang, X. Yang, J. Phys. Chem. B, 2013, 117, 9050−9055.

[18] M. Kollmannsberger, K. Rurack, U. Resch-Genger, J. Daub, J. Phys. Chem. A, 1998, 102, 10211-10220.

[19] K. Rurack, M. Kollmannsberger, U. Resch-Genger, J. Daub, J. Am. Chem. Soc., 2000, 122, 968-969.

[20] L. B. Josefsen, R. W. Boyle, Met Based Drugs., 2008, 2008, 276109.

[21] X.-F. Zhang, J. Zhang, L. Liu, J. Fluoresc. 2014, 24, 819 − 826.

[22] T. Nyokong, Coord. Chem. Rev. 2007, 251, 1707-1722.

[23] N. Epelde-Elezcano, V. Martinez-Martinez, E. PeÇa-Cabrera, C. F. A. Gjmez-Duran, I. L. Arbeloa, S. Lacombe, RSC Adv. 2016, 6, 41991-41998.

[24] M. Kollmannsberger, K. Rurack, U. Resch-Genger, W. Rettig, J. Daub, Chem. Phys. Lett. 2000, 329, 363-369.

[25] P. Van Haver, N. Helsen, S. Depaemelaere, M. Van der Auweraer, F. C. De

Schryver, J. Am. Chem. Soc., 1991, 113(18), 6849-6857.

[26] A. Onkelinx, G. Schweitzer, F. C. De Schryver, H. Miyasaka, and M. Van der Auweraer , T. Asahi, H. Masuhara, and H. Fukumura , A. Yashima, K. Iwai, J. Phys. Chem. A 1997, 101, 5054-5062.

[27] J. Herbich. A. Kapturkiewicz, Chem. Phys. 1991, 158, 143-153.

[28] G. B.Clemans, M. Alemayehu, Tetrahedron Lett., 1993, 34(10), 1563-1566.

ACCEPTED MANUSCRIPT

ACCEPTED MANUSCRIPT

Highlights

- Six 8-(*para*-amino) phenyl substituted BODIPY photosensitizers were prepared.
- They can efficiently generate singlet oxygen in medium polar environments.
- They exhibit high fluorescence quantum yields in nonpolar solvents but low fluorescence quantum yields in polar solvents.
- Both quantum yields for singlet oxygen formation and fluorescence are increased by the methyl in 1 and 7 positions of the BODIPY core.

ACCEPTED MANUSCRIPT